Journal of Materials Research and Technology 33 (2024) 9595–9602

Contents lists available at ScienceDirect

Journal of Materials Research and Technology

journal homepage: www.elsevier.com/locate/jmrt

Application of shot peening to improve fatigue properties via enhancement of precipitation response in high-strength Al–Cu–Li alloys

Michal Jambor [a,*], Libor Trško [b], Ivo Šulák [a], Filip Šiška [a], Sara Bagherifard [c], Mario Guagliano [c], Zuzana Florková [b]

[a] Institute of Physics of Materials, Czech Academy of Sciences, Zizkova 22, Brno, Czech Republic
[b] Research Centre of the University of Zilina, Zilina, Slovak Republic
[c] Politecnico di Milano, Department of Mechanical Engineering, Via la Masa 1, Milano, Italy

ARTICLE INFO

Handling editor: P Rios

Keywords:
Aluminum alloy
Precipitation
Fatigue
Shot peening

ABSTRACT

This paper investigates the role of a hybrid treatment considering severe shot peening as a pre-treatment to age-hardening in enhancing the fatigue properties of an advanced high-strength Al–Cu–Li alloy. The alloy was subjected to severe shot peening with a combination of two different heat treatment regimes, aiming for microstructural modification to promote precipitation of heterogeneously nucleating phases. The effects of different treatments based on combined ageing and severe shot peening on residual stresses, hardness, microstructural characteristics, and fatigue properties were evaluated and critically discussed. The results have shown that in the case of heat treatment regimes at which the formation of heterogeneously nucleating T_1 precipitates occurs, the application of severe shot peening prior to ageing results in significant refinement of strengthening particles, enhancing the fatigue properties in the short and medium fatigue lifetimes.

1. Introduction

Al–Cu–Li alloys offer high mechanical strength while still maintaining sufficient ductility [1–4]. These properties are achieved by the age-hardening (ageing) heat treatments – during which strengthening precipitates are formed in the aluminum matrix. The main strengthening phase in advanced Al–Cu–Li alloys is T_1 (Al_2CuLi), whose particles preferentially nucleate in a heterogeneous manner on the lattice defects [5–7]. Optimal mechanical properties are obtained in the case of advanced Al–Cu–Li alloys through T8 class tempers, which utilize plastic deformation in terms of 2–3 % stretching between solution annealing and ageing. However, due to its nature, the use of T8 tempers is limited to standardized profiles and cannot be applied to parts after forming or shaping processes with complex geometry. The conventional ageing treatments do not reach the optimal mechanical properties comparable to those obtained by the T8 regimes. This opens the question of whether applying any surface strengthening technique followed by age-hardening can improve the local mechanical properties of the surface layer sufficiently to enhance the overall fatigue resistance, or not.

Several studies have proven the positive effect of the severe shot peening (SSP) surface treatment on the fatigue properties of Aluminum alloys, especially in the very high cycle fatigue region [8–11]. A combination of multiple factors induced by SSP contribute to improving fatigue properties; however, the most significant can be considered grain refinement and introduction of compressive residual stresses in the surface and subsurface region after SSP, retarding the fatigue crack initiation, thus enhancing the overall fatigue properties of treated parts [10–13]. Surface hardening is usually considered as a secondary beneficial factor - the severe plastic deformation of the surface introduces lattice defects to the surface and subsurface region. However, besides the positive contribution of surface strengthening to fatigue properties, further enhancement of resistance to foreign object damage was reported [13]. The simplicity of the process, besides its scalability and applicability even for components with complex shapes, makes SSP a suitable candidate for strengthening Al–Cu–Li alloys. Combined with age-hardening performed after surface strengthening, SSP treatment can substitute non-applicable T8 tempers and enhance the overall fatigue properties of high-strength alloys.

In the past, several studies were performed focusing on the possibility of precipitation enhancement by the pre-aging severe plastic

* Corresponding author.
E-mail addresses: jambor@ipm.cz (M. Jambor), libor.trsko@uniza.sk (L. Trško), sulak@ipm.cz (I. Šulák), siska@ipm.cz (F. Šiška), sara.bagherifard@polimi.it (S. Bagherifard), mario.guagliano@polimi.it (M. Guagliano), zuzana.florkova@uniza.sk (Z. Florková).

https://doi.org/10.1016/j.jmrt.2024.11.260
Received 1 October 2024; Received in revised form 15 November 2024; Accepted 27 November 2024
Available online 28 November 2024

deformation [14–20]. An increase in the dislocation density is reported to result in the precipitation of densely populated finer particles. Besides that, due to dislocation interactions, vacancies are emitted, enhancing the diffusion rate and thus affecting the kinetics of precipitation processes [16,20,21]. On the other hand, excessive severe plastic deformation results in the formation of numerous high-angle grain boundaries, which can act as a sink for the solutes and decrease the supersaturation of the solid solution [21]. Despite the unambiguous precipitation enhancement capabilities of the pre-ageing plastic deformation, the effects of these treatments on the mechanical and, especially, fatigue properties are questionable. Only a few studies have focused on the fatigue performance of aluminum alloys with pre-ageing severe plastic deformation applied to the surface [20,22]. Applying such a surface treatment enhances precipitation in the affected region; but on the other hand, it creates significant surface roughness and can cause the creation of various surface and sub-surface discontinuities. Another aspect is residual stress distribution. In many severe plastic deformation techniques, residual stresses are the critical factor responsible for improving the high cycle fatigue performance. The ageing treatment can partially or even fully relieve residual stresses. Increased surface roughness and relieving residual stresses can easily outbalance the positive effects of enhanced precipitation. This underlines the necessity for carefully choosing the pre-ageing severe shot peening parameters to balance plastic deformation intensity with the level of surface damage.

In the present study, SSP was applied as a pre-treatment to age-hardening with the aim of promoting precipitation of the heterogeneously nucleating precipitates. Four series of samples were prepared as shown in Fig. 1. Two different age-hardening heat treatments were chosen – low-temperature (130 °C) and high-temperature (160 °C) regimes, each of them promoting precipitation of the different strengthening particles. For both heat treatment types, two sample series were prepared. In the first series, SSP was applied after solution annealing and before the ageing step. In the second (control) series, SSP was applied after completing age-hardening, which is conventional engineering practice. In the low-temperature regime, the strengthening is mainly governed by copper-rich precipitates such as Guinier-Preston (GP) zones and Θ". These precipitates are formed homogeneously, so their precipitation does not depend on the local dislocation density. On the other hand, the high-temperature heat treatment regime promotes precipitation of T_1 precipitates predominantly nucleating on the dislocations [6,7,23,24]. High dislocation density formed during SSP treatment can promote precipitation of the denser population of finer precipitates in the affected surface zone. The fatigue properties of all four series in the high cycle region were then examined to evaluate if the application of the SSP before ageing can improve global fatigue properties. The results were then discussed in light of the microstructural characterization of the subsurface-affected layers and the evaluation of the residual stresses.

2. Material and experimental methods

Commercially available 2055 alloy was considered as an experimental material. The alloy was delivered as extruded bars with a diameter of Ø 66 mm. Microstructure and nominal chemical composition are shown in Fig. 2. Four series of specimens were machined and subjected to SSP process. In two series, SSP treatment was applied after solution annealing and before ageing (one of the specimen series was subjected to low-temperature heat treatment and the second one to high-temperature heat treatment). In the other two series, the SSP treatment was applied after the heat treatment (again, one series was subjected to the low-temperature heat treatment, and the other was subjected to the high-temperature heat treatment). SSP treatment was applied in all cases with an Almen intensity of 8.9 N and a coverage of 650%. The SSP process parameters were chosen based on our previous studies [10,11] carried out on AW7075 high-strength aluminium alloy, aiming for optimal parameters for high cycle fatigue properties. Such treatment induced severe plastic deformation to the surface layer while the surface damage (cracks and other discontinuities) was kept as low as possible.

Heat treatments were carried out with the following parameters: Low temperature (LoHT) - solution annealing at 520 °C for 1 h followed by water quenching, ageing at 130 °C for 50h, and, High-temperature heat treatment (HiHT) - solution annealing at 520 °C for 1 h followed by water quenching, ageing at 160 °C for 64h. The parameters of the applied heat treatments were chosen based on a parallel study of the heat treatment effect on the microstructure, which is currently being prepared. The heat treatment parameters were chosen to obtain a peak hardness state at a given temperature. Two temperature regimes of 160 °C and 130 °C were selected. The hardening curves for selected temperatures are shown in Fig. 3. The high-temperature regime was chosen in order to obtain peak strength microstructure containing T_1 precipitates, which are the main strengthening phase in the current

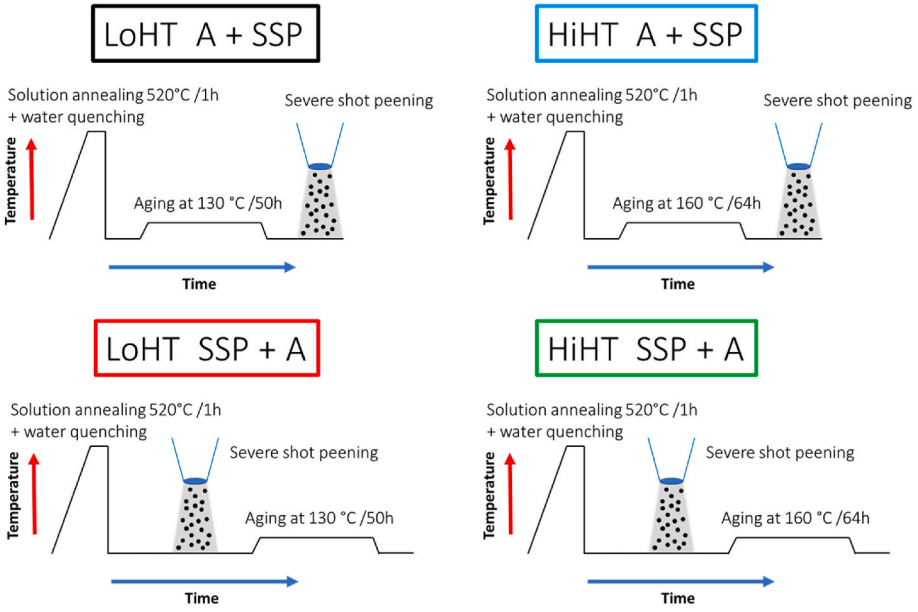

Fig. 1. Schematic view of the tested sample series. Four different series were tested, differing in the ageing temperature and the application of the SSP process before/after aging treatment.

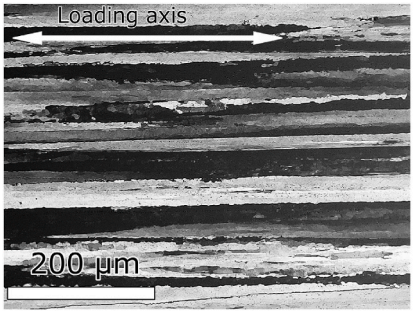

	Cu	Li	Zn	Ag	Mg
wt. %	3.7	1.15	0.5	0.45	0.4
	Zr	Fe	Si	Al	Mn
wt. %	0.1	0.1 max	0.07 max	bal	0.3

Fig. 2. Microstructure and nominal chemical composition of the experimental material, loading axis corresponds with the extrusion direction.

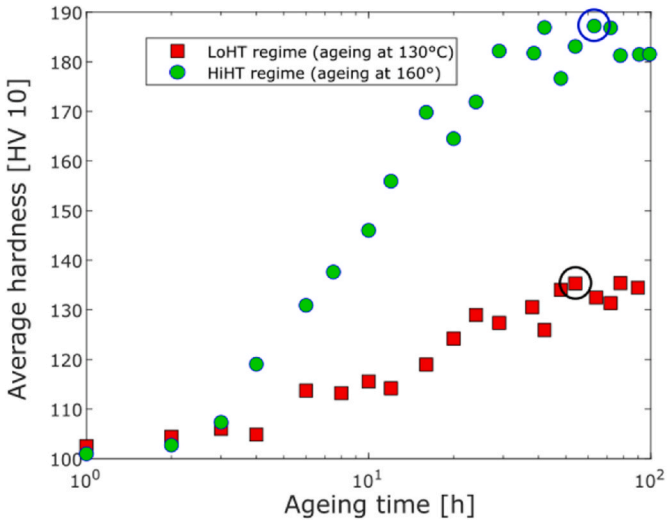

Fig. 3. Hardening curves for chosen temperature regimes. Circles mark chosen peak hardness parameters–50h ageing time for LoHT and 64h for HiHT.

generation of Al–Cu–Li alloys and which nucleate preferentially on lattice defects. The second heat treatment regime was chosen to obtain a microstructure containing a combination of Cu-rich GP zones and θ'' particles, which are the main strengthening phases in Al–Cu–Mg alloys, and where the introduction of additional lattice defect via SSP does not expect to promote their nucleation.

Fatigue tests were carried out on the MTS Acumen12 electrodynamic test system. Tests were performed under a stress control regime with a fully reversible tension-compression loading cycle (R = −1). The testing frequency was 30 Hz, and the tests were terminated if there was no failure in 10^7 loading cycles.

In order to support the obtained fatigue results, residual stresses and surface hardening were examined within not-loaded specimens subjected to the hybrid treatments. In-depth residual stress profiles were examined using X-ray diffraction. A Proto iXRD diffractometer equipped with a Cr X-ray source was used, and the measurements were performed using the $\sin^2\psi$ method, with 6 inclinations between ±40°. Diffraction peaks from {222} planes were collected at 156.9° diffraction angle. To assess the residual stress levels at different depths, electrolytic polishing was used for a gradual removal of a thin surface layer. After each polishing step, the depth of the removed layer was measured via a depth gauge, and the whole process was repeated until the required depth was reached. Due to the strong crystallographic texture of the base material, the residual stress levels could be measured only in the very thin, heavily deformed layer, where the deformation process suppressed the texture. As the effect of suppressed texture gradually disappeared, the results started to show higher scatter. Therefore, the most reliable information on residual stress values was obtained in the surface and near-surface region.

The surface hardening extent was also monitored via nanoindentation measurements. Experiments were conducted using Zwick ZHN nanomechanical machine. The indentation was performed with the Vickers diamond tip, which was force driven and loaded up to 100 mN. The hardness was calculated as the ratio of maximal applied force and indent area at this maximal force. The indent area was estimated using a calibration function depending on the indentation depth measured during loading. The individual indents were placed in a "zigzag" pattern to keep their mutual distance of 40 μm while achieving the spatial resolution of 10 μm in the direction perpendicular to the surface. Measurements were performed at electropolished cross-sections from the surface up to a depth of 250 μm. The surface roughness was evaluated using DSX1000 digital optical microscope. For each specimen, three areas with a size of 380 × 380 μm were scanned, and the areal surface roughness parameters were extracted. The application of a cut-off filter compensated for the curvature of the sample gauge length. Final surface roughness parameters for each examined state were then calculated as an average value from all three measurements.

The microstructure of the subsurface region was examined with the help of transmission electron microscopy. Firstly, lamellas were prepared from all four specimen series using the focused ion beam technique (FIB). The approximate dimensions of the lamellas were 25×15 μm, and they were oriented in a way to show the gradual microstructural changes from the surface to 25 μm depth below the surface. Microstructure was then observed using a Thermofisher Talos F200i transmission electron microscope. The size of the strengthening particles was evaluated at a distance of 10 μm from the surface of the specimens. In the case of the LoHT, images for precipitate evaluation were taken close to the zone axis <001>, while for the HiHT series, specimens were oriented close to the <011> zone axis. The size of the particles in edge-on orientation was measured, and the average values were calculated.

3. Results

Results of the fatigue tests are shown in Fig. 4. Both series of LoHT exhibited similar behavior at the short and medium fatigue lifetimes. However, for longer fatigue lifetimes, series with the SSP process applied after age-hardening showed superior fatigue properties compared to series with the SSP applied before ageing. Based on this, it can be stated that in the case of LoHT, the application of severe plastic deformation before ageing treatment has no beneficial effect. Different behavior was recorded for the HiHT series. In this case, specimens with SSP applied before ageing showed superior fatigue properties at short and medium fatigue lifetimes. At long fatigue lifetimes, the differences between both HiHT series diminished. Application of SSP before ageing in the case of HiHT was therefore beneficial in certain regions of the fatigue lifetimes. As several factors contribute to the fatigue properties of SSP-treated specimens, each was separately analyzed in the following sections.

At first, residual stress depth profiles were evaluated, as shown in Fig. 5. Additional measurements were performed on the specimens after

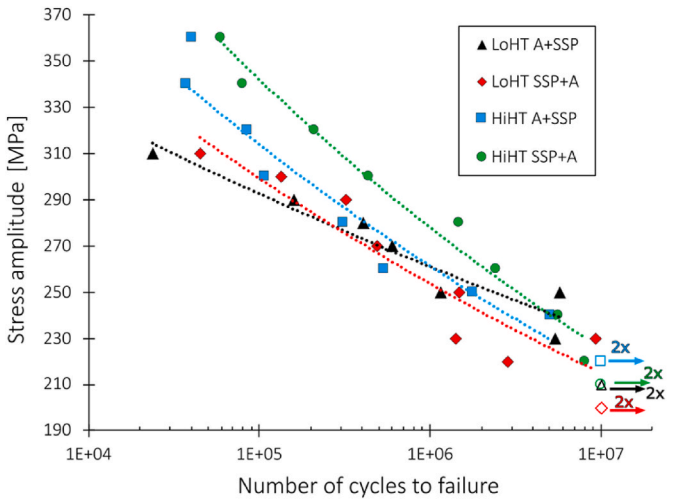

Fig. 4. Results of the fatigue tests in the form of S–N curves. While in the case of LoHT, no beneficial effect of introducing the SSP process before ageing is visible, in the HiHT series, application of the SSP before ageing improves fatigue properties at short and medium fatigue lifetimes.

solution annealing and SSP without any additional ageing treatment. This allowed monitoring of possible relaxation during applied heat treatments. In all examined series, the SSP application resulted in the formation of compressive residual stresses in the subsurface region. Fig. 5a shows residual stress depth profiles measured on the LoHT series. No significant differences were recorded between LoHT SSP + A, LoHT A + SSP, and the reference Solution annealed + SSP series, suggesting minimal residual stress relaxation during the applied low-temperature heat treatment. Different behavior was recorded for the HiHT series (Fig. 5b). In the case of the HiHT A + SSP, the magnitude of the compressive residual stresses was similar to the reference state (solution annealed + SSP), but the affected zone was very shallow. This can be explained by the higher initial hardness of the HiHT A + SSP series. However, the residual stress profile of the HiHT SSP + A series showed a significant drop compared with the reference ones, whereas the depth of the introduced residual stresses was greater when compared to the HiHT A + SSP series. It is expected that the ageing temperature of 160 °C is sufficiently high for a partial relaxation of residual stresses induced by SSP. Similarly to the residual stress distribution, differences were also recorded in the surface roughness. Results of the optical surface roughness measurements are shown in Fig. 6 and Table 1. The higher initial hardness of LoHT A + SSP and HiHT A + SSP series resulted in lower surface roughness compared to the series with SSP applied before ageing.

The hybrid treatment resulted in distinctive differences in the mechanical properties as evaluated with the help of the nanoindentation measurements (see Fig. 7). In all cases, the SSP process resulted in the hardening of the surface region, while the extent of the hardening and the depth of the affected layer depended on the applied regime of the hybrid treatment. In the case of LoHT SSP + A combined treatment, a steep increase in hardness was recorded in the surface layer up to the depth of approximately 50 μm, after which the hardness levels reached the average hardness values of the core. A similar situation was recorded for the LoHT A + SSP series. The maximal hardness in the proximity to the surface was comparable to that of LoHT SSP + A. However, at higher distances from the surface, hardness values slightly exceeded the average hardness in the core, and that of the LoHT SSP + A. A possible explanation for this observation could be a decrease in the dislocation density after SSP by partial annealing of the microstructure when the heat treatment is applied after the SSP.

Hardness values in the HiHT series were significantly higher than in the LoHT series, highlighting the larger hardening potential of the strengthening phases forming during the HiHT regime. Peak hardness in the near-surface region was similar in both HiHT series, with moderate hardness decreasing towards the core. At larger distances from the surface, the HiHT SSP + A series exhibited slightly higher hardness than the HiHT A + SSP series, but due to the considerably large scatter of the experimental data, it is impossible to properly quantify the difference.

The application of SSP significantly modified the microstructure in the near-surface region (Figs. 8 and 9). Within the LoHT series, intensive plastic deformation induced by SSP resulted in very high dislocation density within the whole examined area. In both LoHT variants, a fine nanocrystalline layer with a depth of 2–3 μm was recorded. Densely populated strengthening particles were, in the case of LoHT, identified as GP zones and θ'', precipitating in the form of laths on $\{001\}_\alpha$ planes. A comparison of images taken at a distance of 10 μm from the surface did not reveal any differences in shape or size of the strengthening particles between the LoHT A + SSP and LoHT SSP + A series.

Microstructures of the HiHT series in the surface and subsurface regions are shown in Fig. 8. Similarly to the LoHT series, both HiHT specimens exhibited very high dislocation density within the examined area. Besides that, a fine nanocrystalline layer was present near the surface. In both HiHT series, no intergranular precipitates were present in the nanocrystalline surface layer. The HiHT SSP + A series exhibited pronounced grain boundary precipitation (Fig. 8c–f). Distinctive differences were recorded in the size of the strengthening particles. Microstructure was analyzed at a distance of 10 μm from the surface, emphasizing the appearance of the main strengthening phase Al_2CuLi

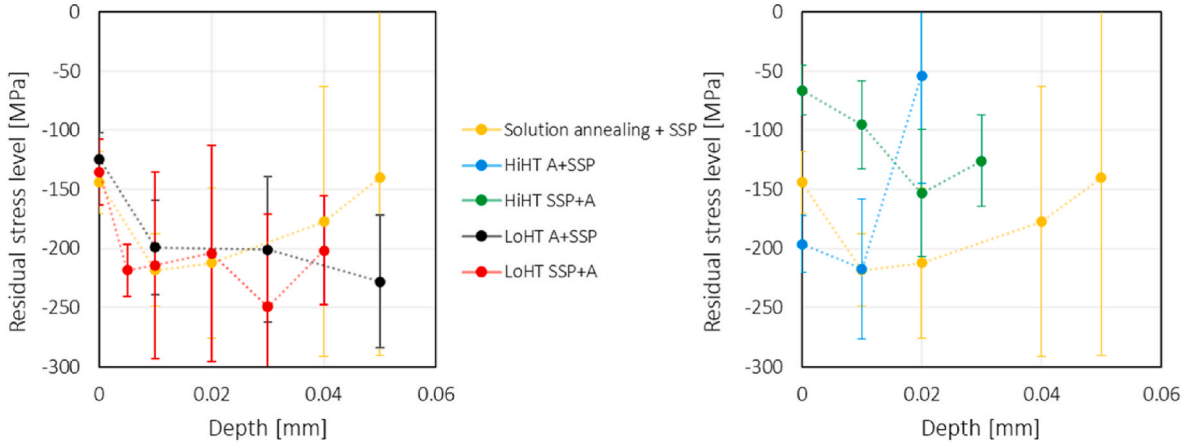

Fig. 5. Residual stress depth profiles of all examined series. Compressive residual stresses in the subsurface region induced by the SSP process were recorded in all series.

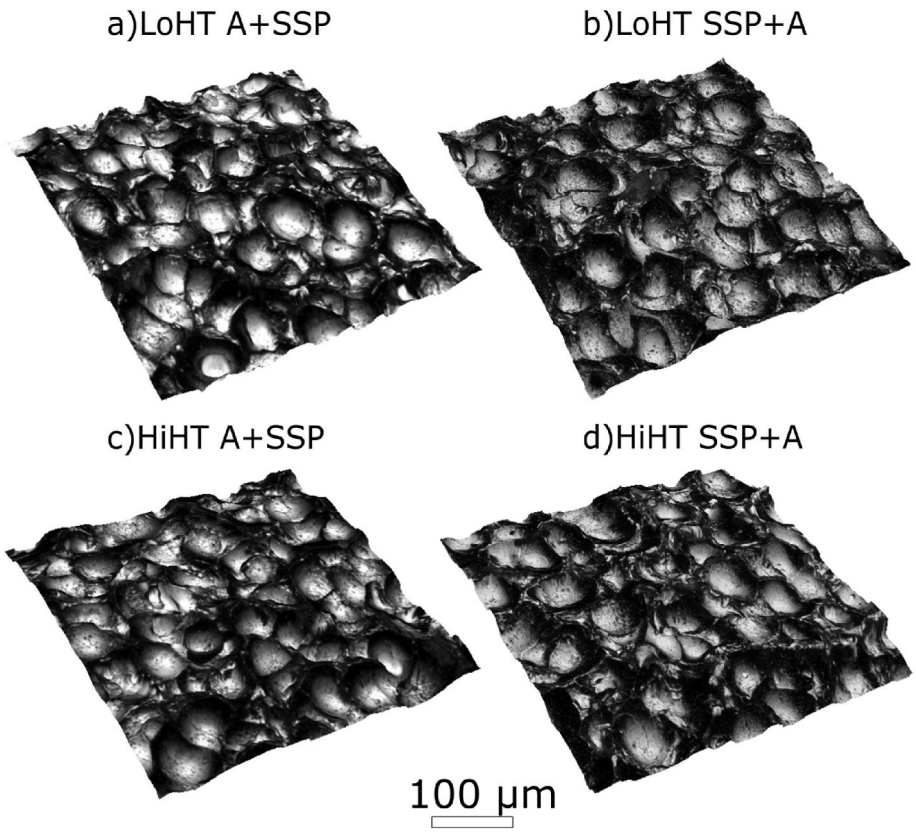

Fig. 6. Comparison of the surface quality of examined series. Quantitative data of the areal surface roughness are shown in Table 1.

Table 1
Area surface roughness parameters of all tested sample series.

Series	Sa [μm]	Sz [μm]	Sp [μm]	Sv [μm]	Sq [μm]
LoHT A + SSP	2.192	18.55	10.081	8.47	2.732
LoHT SSP + A	2.41	19.532	8.718	10.813	2.979
HiHT A + SSP	2.045	16.138	8.369	7.768	2.55
HiHT SSP + A	2.313	17.948	7.733	10.215	2.881

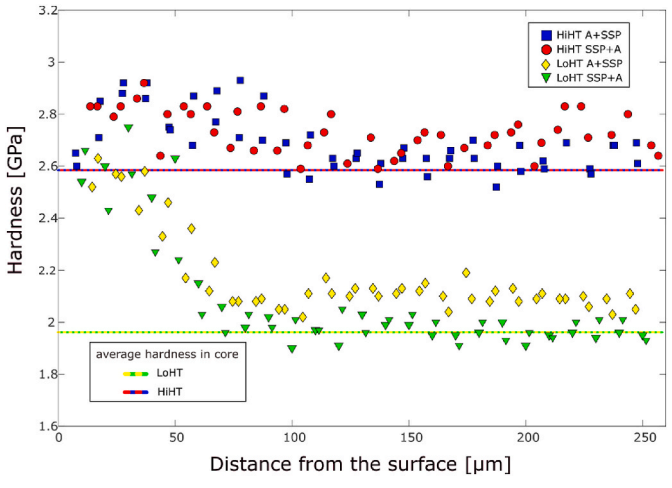

Fig. 7. Results of the nanoindentation measurement show hardness evolution with increasing distance from the surface.

(T_1). In the case of the HiHT A + SSP series, the average particle size was measured to be (122.4 ± 39.4) nm. Treatment applied to the HiHT SSP + A series resulted in significant refinement of the precipitates, as the average precipitate size was revealed to be (37.1 ± 10.2) nm. The results indicate that the introduction of the SSP process before ageing thus promotes nucleation of the precipitates, resulting in the formation of very fine dispersed strengthening particles.

4. Discussion

The performed fatigue tests revealed noticeably different effects of SSP application in combination with ageing on the fatigue properties of 2055 alloy. As the mechanisms are significantly different with respect to the ageing temperature and the type of precipitating particles, the results are discussed here individually for the low-temperature and high-temperature age-hardened series.

4.1. LoHT series

In the case of applied LoHT treatment regimes, the introduction of SSP before ageing did not show any benefits in terms of high cycle fatigue properties. Moreover, a deterioration of the fatigue resistance was recorded, especially at the longer fatigue lifetimes. LoHT SSP + A exhibited moderate enhancement of the fatigue properties at shorter lifetimes, closer to the low cycle fatigue region, while LoHT A + SSP was superior in the regions at longer lifetimes, closer to the fatigue limit. As the residual stresses and the microstructure observations did not reveal any significant differences, the main aspects are the surface state and the difference in substrate hardness prior to the SSP process. A softer matrix when SSP was applied before ageing resulted in the slightly higher surface roughness of the substrate, with negative consequences for the fatigue resistance, highlighted at longer fatigue lifetimes. The slightly higher hardness of LoHT A + SSP at larger distances from the surface suggests that in the case of LoHT SSP + A, a partial recovery occurred during applied ageing. However, the residual stress profiles did not reveal any significant differences. Based on the performed experiments,

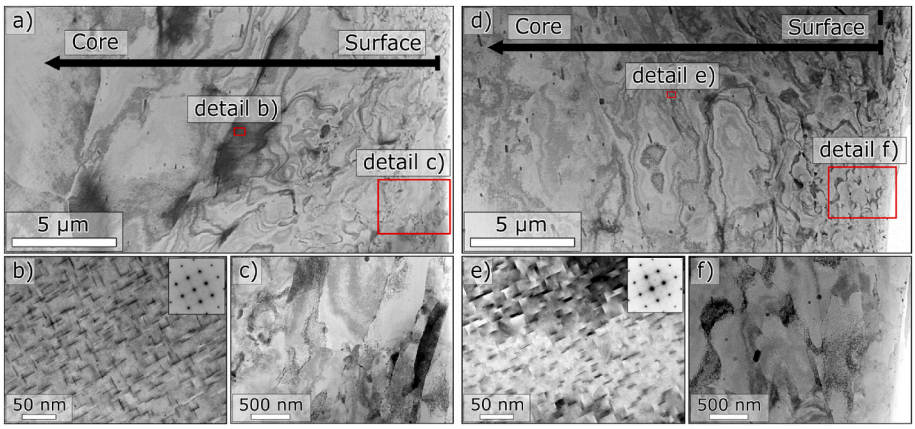

Fig. 8. Microstructure of LoHT A + SSP (a–c) and LoHT SSP + A (d–f) series (STEM-BF). High dislocation density is visible in both series, with a nanocrystalline layer near the surface (c, f). Microstructure contains fine dispersion of strengthening precipitates of Al_2Cu phase, with no difference in size or shape between the examined series (b, e).

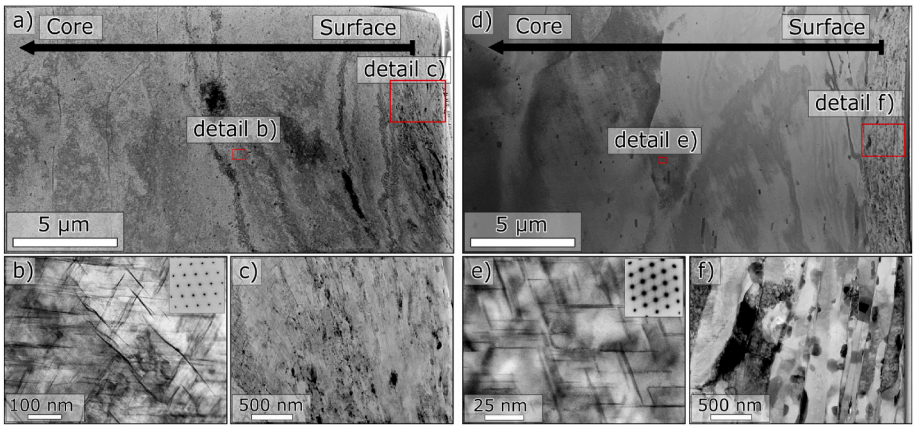

Fig. 9. Microstructure of HiHT A + SSP (a–c) and HiHT SSP + A (d–f) series. Like the LoHT series, both HiHT series exhibited high dislocation density and a fine nanocrystalline layer near the surface (c, f). The size of the strengthening precipitates (Al_2CuLi) was distinctively different (b, e), with an average size of the particles within HiHT A + SSP more than three times larger than in the HiHT SSP + A series.

it can be concluded that in the case of the LoHT regimes of heat treatment, the application of SSP before ageing does not bring any advantage in improving HCF properties. Trying to generalize this statement, it seems that if there is no modification of the structure and morphology of the precipitates, the conventional SSP process, applied after finished heat treatment, provides better fatigue properties of the treated components. Application of SSP before ageing can enhance diffusion, thus reducing the time required for ageing [25]. Nevertheless, this effect is considered almost negligible in the present study.

4.2. HiHT series

In the case of the HiHT treatment regimes, the application of the SSP before ageing improved the fatigue properties within the whole tested region, except for the zone close to the fatigue limits. This behavior differs from the results of the conventional application of SSP on Al alloys, as usually more significant improvements are reported at longer fatigue lifetimes [8,11,26,27]. The residual stress profiles revealed differences between the HiHT series. Conventional application of the SSP (HiHT A + SSP) resulted in the maximal compressive stresses forming at a depth of about 0.01 mm, followed by a rapid decline in magnitude. On the other hand, when SSP was applied before ageing (HiHT SSP + A), the residual stresses were induced into larger depths, although at a lower magnitude. When comparing the residual stress profile of the HiHT SSP + A series and an additional control sample with SSP applied after solution annealing, it is evident that ageing treatment relieved a significant part of the introduced residual stresses (Fig. 5). In light of the in-depth residual stress profiles, it was noticed that the HiHT SSP + A series exhibited improved fatigue properties despite the reduced overall level of the compressive residual stresses in the subsurface region. While in the case of conventional application of SSP, the residual stresses and surface grain refinement seemed to be the key factors determining fatigue properties [8,12]; the results indicate that other factors (deformation-stimulated precipitation) played a dominant role since also both samples exhibited similar surface grain refinement.

Nanoindentation revealed that the hardness in the affected zone of the HiHT series was significantly higher than the LoHT series. This can be attributed to the different nature of the strengthening particles, which, in the case of HiHT, provided more effective obstacles for dislocation movement. Focusing on the HiHT series itself, both variants exhibited similar hardness profiles. Further from the surface, the HiHT SSP + A series' hardness was slightly higher than that of HiHT A + SSP. However, due to the overall large scatter of the experimental data, this difference was insignificant.

More distinct differences were observed in the microstructure when the appearance at a distance of 10 μm from the surface was compared. The high dislocation density induced by the SSP process resulted in the precipitation of the very fine T_1 particles in the HiHT SSP + A series. The average size of the particles was 37.1 ± 10.2 nm at a distance of 15 μm from the surface. In the same area, the average size of T_1 particles in the

HiHT A + SSP series was 122.4 ± 39.4 nm. Significant refinement of the strengthening particles appeared to be the decisive factor responsible for improving the fatigue properties. It is worth noting that such a significant difference did not show a more pronounced difference in the hardness of both series. It is believed that the finer precipitates mainly enhanced yield strength, while the overall hardness may correspond better with the changes in ultimate strength.

It is generally known that finer and more densely populated precipitates provide a more effective barrier for dislocation movement and exhibit higher resistance to the crack initiation and short crack propagation stage [28,29]. Thus, the diminishing of the positive effect at longer lifetimes is attributed to the differences in the residual stress field, whose partial relaxation depends on whether the ageing is applied before/after SSP treatment. Based on numerous studies, in the case of SSP application on metallic materials, enhancement of the fatigue properties is mainly attributed to the presence of the compressive surface residual stress fields, and the effect is more pronounced at longer fatigue lifetimes close to the fatigue limit. Considering the negative impact of lower initial hardness, the related high surface roughness and the partial relaxation of the residual stresses in HiHT SSP + A, enhancement of the fatigue properties at shorter and medium fatigue lifetimes is given by the strengthening particle refinement. These results provide a promising future prospect for the application of surface-strengthening methods in the case of advanced Al–Cu–Li alloys. The mentioned negative effect of this treatment can be suppressed or reduced, for example, via the application of a two-step SSP process to improve the surface quality or by introducing another SSP step after the hybrid treatment with the potential of further improvement of the fatigue properties.

5. Conclusions

The obtained results indicate that the application of the severe shot peening process as a pre-treatment before age-hardening is beneficial for fatigue properties when the strengthening particles tend to heterogeneously nucleate on introduced lattice defects, which is the case of high-temperature heat treatment regime in Al–Cu–Li alloys. Application of SSP before ageing results in the formation of a finer and denser population of T_1-strengthening particles. Conversely, no beneficial effect regarding particle distribution was recorded in the case of low-temperature heat treatment, where the precipitation of Cu-rich Al_2Cu particles dominates, and the applied SSP process did not enhance their precipitation.

Specimens with the severe shot peening process applied before high-temperature ageing showed superior fatigue resistance in short and medium fatigue lifetimes, compared to the series with shot peening conventionally applied after finished age-hardening. At long fatigue lifetimes, the superiority of shot peened + aged samples diminished, and both series exhibited similar properties.

Data availability

All data are accessible via the Zenodo repository: 10.5281/zenodo.13484094.

Declaration of competing interest

The authors declare that they have no known competing financial interests or personal relationships that could have appeared to influence the work reported in this paper.

Acknowledgement

This publication was supported by the project “Mechanical Engineering of Biological and Bio-inspired Systems”, funded as project No. CZ.02.01.01/00/22_008/0004634 by Programme Johannes Amos Commenius, call Excellent Research.

References

[1] Wu L, Li X, Wang H. The effect of major constituents on microstructure and mechanical properties of cast Al-Li-Cu-Zr alloy. Mater Char 2021;171:110800.
[2] Chen X, Ma X, Xi H, Zhao G, Wang Y, Xu X. Effects of heat treatment on the microstructure and mechanical properties of extruded 2196 Al-Cu-Li alloy. Mater Des 2020;192:108746.
[3] Deschamps A, Decreus B, De Geuser F, Dorin T, Weyland M. The influence of precipitation on plastic deformation of Al–Cu–Li alloys. Acta Mater 2013;61(11):4010–21.
[4] Abd El-Aty A, Xu Y, Guo X, Zhang S-H, Ma Y, Chen D. Strengthening mechanisms, deformation behavior, and anisotropic mechanical properties of Al-Li alloys: a review. J Adv Res 2018;10:49–67.
[5] Li JF, Chen YL, Zhang XH, Zheng ZQ. Role of pre-deformation on aging precipitation behavior of Al-Cu-Li alloys. Mater Sci Forum 2017;877:180–7.
[6] Li J-F, Ye Z-H, Liu D-Y, Chen Y-L, Zhang X-H, Xu X-Z, Zheng Z-Q. Influence of pre-deformation on aging precipitation behavior of three Al–Cu–Li alloys. Acta Metall Sin 2017;30(2):133–45.
[7] Xie B, Huang L, Xu J, Su H, Zhang H, Xu Y, Li J, Wang Y. Effect of the aging process and pre-deformation on the precipitated phase and mechanical properties of 2195 Al–Li alloy. Mater Sci Eng, A 2022;832:142394.
[8] Jambor M, Trško L, Klusák J, Fintová S, Kajánek D, Nový F, Bokůvka O. Effect of severe shot peening on the very-high cycle notch fatigue of an AW 7075 alloy. Metals 2020.
[9] Hadzima B, Nový F, Trško L, Pastorek F, Jambor M, Fintová S. Shot peening as a pre-treatment to anodic oxidation coating process of AW 6082 aluminum for fatigue life improvement. Int J Adv Des Manuf Technol 2017;93(9):3315–23.
[10] Trško L, Fintová S, Nový F, Bokůvka O, Jambor M, Pastorek F, Florková Z, Oravcová M. Study of relation between shot peening parameters and fatigue fracture surface character of an AW 7075 aluminium alloy. Metals 2018.
[11] Trško L, Guagliano M, Bokůvka O, Nový F, Jambor M, Florková Z. Influence of severe shot peening on the surface state and ultra-high-cycle fatigue behavior of an AW 7075 aluminum alloy. J Mater Eng Perform 2017;26(6):2784–97.
[12] Unal O, Maleki E, Karademir I, Husem F, Efe Y, Das T. Effects of conventional shot peening, severe shot peening, re-shot peening and precised grinding operations on fatigue performance of AISI 1050 railway axle steel. Int J Fatig 2022;155:106613.
[13] Wang L, Zhou L, Liu L, He W, Pan X, Nie X, Luo S. Fatigue strength improvement in Ti-6Al-4V subjected to foreign object damage by combined treatment of laser shock peening and shot peening. Int J Fatig 2022;155:106581.
[14] Mohammadi A, Enikeev NA, Murashkin MY, Arita M, Edalati K. Developing age-hardenable Al-Zr alloy by ultra-severe plastic deformation: significance of supersaturation, segregation and precipitation on hardening and electrical conductivity. Acta Mater 2021;203:116503.
[15] Zuo J, Hou L, Shi J, Cui H, Zhuang L, Zhang J. Effect of deformation induced precipitation on grain refinement and improvement of mechanical properties AA 7055 aluminum alloy. Mater Char 2017;130:123–34.
[16] Zhao Y, Liu J, Topping TD, Lavernia EJ. Precipitation and aging phenomena in an ultrafine grained Al-Zn alloy by severe plastic deformation. J Alloys Compd 2021;851:156931.
[17] Mirzakhani B, Payandeh Y. Combination of sever plastic deformation and precipitation hardening processes affecting the mechanical properties in Al–Mg–Si alloy. Mater Des 2015;68:127–33.
[18] Vaseghi M, Kim HS. A combination of severe plastic deformation and ageing phenomena in Al–Mg–Si Alloys. Mater Des 2012;36:735–40.
[19] García-Infanta JM, Swaminathan S, Cepeda-Jiménez CM, McNelley TR, Ruano OA, Carreño F. Enhanced grain refinement due to deformation-induced precipitation during ambient-temperature severe plastic deformation of an Al–7%Si alloy. J Alloys Compd 2009;478(1):139–43.
[20] Maurel P, Weiss L, Grosdidier T, Bocher P. How does surface integrity of nanostructured surfaces induced by severe plastic deformation influence fatigue behaviors of Al alloys with enhanced precipitation? Int J Fatig 2020;140:105792.
[21] Feng Z, Luo X, Chen Y, Chen N, Wu G. Surface severe plastic deformation induced solute and precipitate redistribution in an Al-Cu-Mg alloy. J Alloys Compd 2019;773:585–96.
[22] Ludian T, Wagner L. Effect of age-hardening conditions on high-cycle fatigue performance of mechanically surface treated Al 2024. Mater Sci Eng, A 2007;468–470:210–3.
[23] Dorin T, Deschamps A, Geuser FD, Sigli C. Quantification and modelling of the microstructure/strength relationship by tailoring the morphological parameters of the T1 phase in an Al–Cu–Li alloy. Acta Mater 2014;75:134–46.
[24] Prasad NE, Gokhale A, Wanhill RJH. Aluminum-lithium alloys: processing, properties, and applications. Butterworth-Heinemann 2013.
[25] Deschamps A, De Geuser F, Horita Z, Lee S, Renou G. Precipitation kinetics in a severely plastically deformed 7075 aluminium alloy. Acta Mater 2014;66:105–17.
[26] Benedetti M, Fontanari V, Bandini M, Savio E. High- and very high-cycle plain fatigue resistance of shot peened high-strength aluminum alloys: the role of surface morphology. Int J Fatig 2015;70:451–62.

[27] González J, Bagherifard S, Guagliano M, Fernández Pariente I. Influence of different shot peening treatments on surface state and fatigue behaviour of Al 6063 alloy. Eng Fract Mech 2017;185:72–81.
[28] Lindigkeit J, Gysler A, Lütjering G. The effect of microstructure on the fatigue crack propagation behavior of an Al-Zn-Mg-Cu alloy. Metall Trans A 1981;12(9):1613–9.
[29] Wang S, Li L, Chen G, Li F, Peng S, Zeng X, Li J, Zhang Y, Li R, Fang Q. Modeling the effect of precipitation spatial geometry and size distribution on the yield strength of aluminum alloys. Acta Mech 2023;234(9):4323–42.